

Obtaining Static Structural Stiffness from Modal Tests

Robson Geremias Macedo; José Roberto de França Arruda

Universidade Estadual de Campinas - UNICAMP

Faculdade de Engenharia Mecânica - FEM

Departamento de Mecânica Computacional - DMC

Rua Mendeleev, s/n - Cidade Universitária "Zeferino Vaz", Barão Geraldo - Campinas - SP - Brazil

Abstract: In the automotive industry, both static and dynamic (modal analysis) tests are currently performed to characterize structural behavior during the development phase of parts of a new vehicle. In general, to characterize static structural stiffness, static tests are performed. These static tests are more elaborate to implement than state-of-the-art modal tests. Thus, this article investigates the possibility of using modal test results to obtain static stiffness. The static behavior appears in the Frequency Response (FRF) curves at the origin. However, as the quality of the estimated FRF at zero frequency is usually poor, a synthesized value obtained by modal superposition must be used instead. The advantage of the procedure comes from the fact that dynamic tests are faster and cheaper. The method is validated using a Finite Element model of a simple structure.

Keywords: *stiffness, dynamic, static, structural, modal*

NOMENCLATURE

m = lumped mass, kg
 c = lumped damping, N/(m/s)
 k = lumped stiffness, N/m
 u = displacement, m
 ω = angular frequency, rad/s

E = Young's modulus, Pa
 I = inertia of the cross-section, m⁴
 v = transversal displacement, m
 ρ = mass density, kg/m³
 A = cross-section area, m²

j = imaginary number, $\sqrt{-1}$

N = total number of modes

INTRODUCTION

Evaluations of the static and dynamic stiffness (modal analysis) are performed during the development of car bodies and other structural parts of vehicles. The results of these evaluations are directly related to vehicle comfort, handling and product life. With this purpose, static and dynamic tests are performed searching for satisfactory results that comply design specifications. Each one of these tests requires dedicated equipment and special devices as well as highly qualified staff.

Static tests require specific devices used to guarantee movements of required degrees of freedom. In the majority of cases, these devices are only used in a specific experimental procedure and exclusively for a specific structure. Moreover, depending on the stiffness of the tested structure, the application of relatively high forces needs extra resources, such as hydraulic or pneumatic actuators. The installation of this equipment and the instrumentation on the structure under test requires a lot of time of man power. Besides, there is a variability of standards and procedures among automotive companies which makes comparisons between results very difficult. The consistency of test results is questionable because it is very difficult to guarantee that the degrees of freedom are the same.

Dynamic tests - and experimental modal analysis is an example - present some advantages over static tests: resources, such as the necessary instrumentation, devices and infrastructure are simpler to be implemented and are usually less expensive; they present greater robustness of the test results and they are easier to reproduce, since it is relatively easy to guarantee the free-free condition of a structure. As disadvantages it can be mentioned the necessity of more powerful computational resources for signal processing and complex calculations during the analysis phase. However, nowadays, the abundance of the available resources made this disadvantage less critical.

The easiness of implementation and viability of dynamic tests in comparison to static tests have taken engineers and researchers of the automotive industry to investigate the possibility of obtaining static results from dynamic tests. Recent works have appeared trying to explore this idea in many implementations (Rediers et al., 1998 and Griffiths et al., 2001). In this paper, we show how such results can be achieved. We initiate with the theoretical basis of the method and apply it to a lumped parameter system. Then we derive the analytical solution for a simple structure with distributed parameters (a continuum beam) and extract the static stiffness using a finite element model of this structure. These are preliminary results of a study of the robustness of the proposed method with respect to modal parameter uncertainties.

Theoretical basis

Obtaining the static stiffness from a dynamic modal test is possible because the information of the former is contained in the result of the latter. The Frequency Response Function (FRF) estimated in the modal test, for example, brings this information in the DC frequency. The theory presented hereafter is based in this principle.

One-Degree-of-Freedom Lumped Parameter System

The lumped parameter system model is widely used in the vibration literature to describe with a very simple dynamic model the characteristics of a given structure in a given frequency range. Consider a system of this type under a force $p(t)$ with the equation of motion given by Eq. (1).

$$m\ddot{u}(t) + c\dot{u}(t) + ku(t) = p(t) \quad (1)$$

Applying the Fourier Transform on both sides of the Eq. (1) and isolating the ratio $H(\omega) = U(\omega) / P(\omega)$ we obtain the analytical expression for the FRF in the frequency domain:

$$H(\omega) = \frac{U(\omega)}{P(\omega)} = \frac{1}{(k - \omega^2 m) + j\omega c} \quad (2)$$

With $\omega=0$ in Eq. (2) the static compliance (or receptance) of the spring, $1/k$, is obtained.

Clamped-Free Beam: Obtaining the Static Compliance from the Analytical Modal Solution

Consider an Euler-Bernoulli clamped-free beam of length L as shown in Fig. 1. The equation of motion for transversal vibrations without distributed load is given by (Craig, 1981):

$$(EIv''') + \rho Av\ddot{v} = 0 \quad (3)$$

where v'' is the second spatial derivative of v .

Assuming a harmonic solution, Eq. (3) becomes:

$$(EIV''') - \rho A\omega^2 V = 0 \quad (4)$$

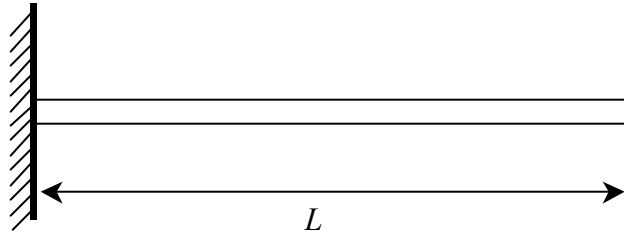


Figure 1 - Euler-Bernoulli clamped free beam

Equation (4) can still be simplified considering a uniform beam:

$$\frac{d^4 V}{dx^4} - \lambda^4 V = 0 \quad (5)$$

where:

$$\lambda^4 = \frac{(\rho A\omega^2)}{EI} \quad (6)$$

The general solution of Eq. (5) can be written in the form:

$$V(x) = C_1 \sinh(\lambda x) + C_2 \cosh(\lambda x) + C_3 \sin(\lambda x) + C_4 \cos(\lambda x) \quad (7)$$

where C_1 , C_2 , C_3 and C_4 are constants to be determined from the boundary conditions.

Applying the boundary conditions in Eq. (7) we obtain a system of equations whose solution is non trivial only in the cases where:

$$\cos(\lambda L)\cosh(\lambda L)+1=0 \quad (8)$$

The roots of Eq. (8) are the eigenvalues λ_r multiplied by the beam length, L . These roots cannot be obtained in closed form and they must be calculated by numerical methods (Chang and Craig, 1969).

Once the roots λ_r are known, we are able to determine the natural frequencies for each mode from the Eq. (6), and the modal shape is given by:

$$V_r(x) = C\{\cosh(\lambda_r x) - \cos(\lambda_r x) - k_r [\sinh(\lambda_r x) - \sin(\lambda_r x)]\} \quad (9)$$

where C is an arbitrary constant and:

$$k_r = \frac{\cosh(\lambda_r L) + \cos(\lambda_r L)}{\sinh(\lambda_r L) + \sin(\lambda_r L)} \quad (10)$$

The modal mass m_r is calculated from the equation:

$$m_r = \rho A \int_0^L V_r^2(x) dx \quad (11)$$

With these, it is possible to calculate the dynamic compliance of mode r between two points of the beam, x_1 and x_2 , from (Ewins, 1984):

$$H_{x_1 x_2}^r = H^r(\omega, x_1, x_2) = \frac{V_r(x_1)V_r(x_2)}{m_r(\omega_r^2 - \omega^2)} \quad (12)$$

The modal superposition is obtained from Eq. (12) when the contributions of the N modes are added up:

$$H_{x_1 x_2} = H(\omega, x_1, x_2) = \sum_{r=1}^N \frac{V_r(x_1)V_r(x_2)}{m_r(\omega_r^2 - \omega^2)} \quad (13)$$

We are interested in the static compliance of the beam free end. Therefore, making $\omega = 0$ and $x_1 = x_2 = L$ in Eq. (13), results:

$$H_{LL} = H(0, L, L) = \sum_{r=1}^N \frac{V_r^2(L)}{m_r \omega_r^2} \quad (14)$$

Table 1 presents the results for the natural frequencies, Eq. (6), the modal shapes, Eq. (9), the modal masses, Eq. (11), the static compliance for each mode at the beam free end, Eq. (12) and the sum of these compliances, Eq. (14), up to the tenth mode.

Table 1 - Results for the clamped-free beam using the analytical solution

Mode r	Natural frequency ¹ ω_r	Modal shape ² $V_r(L)$	Modal mass ³ m_r	Static compliance for each mode ⁴ $H_r(0, L, L)$	Compliance Sum ⁴ $\sum_{k=1}^r H_k(0, L, L)$
1	3.5160	2.0	0.96037	3.235627e-01	0.3235627
2	22.0347	-2.0	0.96128	8.238785e-03	0.3318015
3	61.6972	2.0	0.96209	1.050821e-03	0.3328523
4	120.9019	-2.0	0.96293	2.736488e-04	0.3331260
5	199.8595	2.0	0.96377	1.001406e-04	0.3332261
6	298.5555	-2.0	0.96461	4.487554e-05	0.3332710
7	416.9908	2.0	0.96545	2.300420e-05	0.3332940
8	555.1652	-2.0	0.96629	1.297823e-05	0.3333070
9	713.0789	2.0	0.96712	7.866559e-06	0.3333148
10	890.7318	-2.0	0.96796	5.041573e-06	0.3333199

¹ - normalized using $\frac{1}{L^2} \left(\frac{EI}{\rho A} \right)^{1/2}$; ² - for $C=1$; ³ - normalized using ρA ; ⁴ - normalized using $\frac{L^3}{EI}$.

It can be noticed that the sum of the modal compliances converges to the known result of the static compliance of a clamped-free beam with a concentrated load applied at the free end ($L^3/3EI$). Also, it can be verified that the contribution of each mode falls monotonically, as shown in Fig. 2. In this case, near 97% of the static compliance at the beam free end is due to the contribution of the first mode alone. This evidence allows us to determine the minimum number of modes that should be used to achieve a desired accuracy for the static compliance.

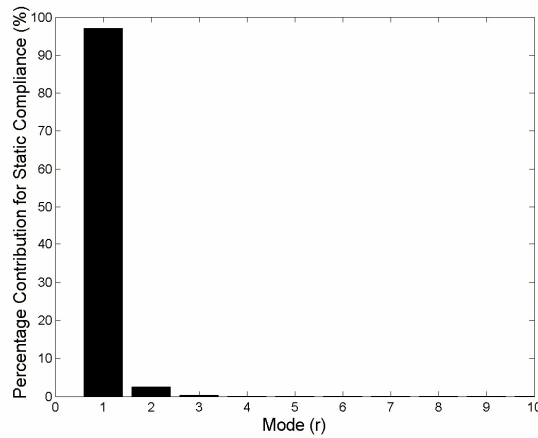


Figure 2 - Modal contribution to static compliance - analytical solution

FINITE ELEMENT MODEL

With the purpose of verifying if the results achieved using the analytical solution can be obtained using numerical models, which can be applied to more complex structures and to create a numerical simulation environment to investigate the method, a finite element (FE) model using Euler-Bernoulli beam elements (Craig, 1981) was implemented. A clamped-free beam and a free-free beam were investigated. In the first one, we intended to validate the numerical implementation by comparing results these results with the analytical. The second case was taken as a more realistic example for the proposed approach that uses the results of a modal test of a free-free structure for the calculation of the static deformation caused by static efforts with the structure under a given condition of restriction.

Clamped-Free Beam

In this implementation the boundary conditions were applied in agreement with Fig. 1, that is, the degrees-of-freedom of one of the end nodes was clamped. Global mass and stiffness matrices were assembled, eigenvalues and eigenvectors were calculated and modal synthesis and modal superposition were performed. Figure 3(a) presents the beam modal shapes and Fig. 3(b) the dynamic compliance at the free end ($x=L$) obtained for the first three modes of the beam. The simulation was performed using 50 elements.

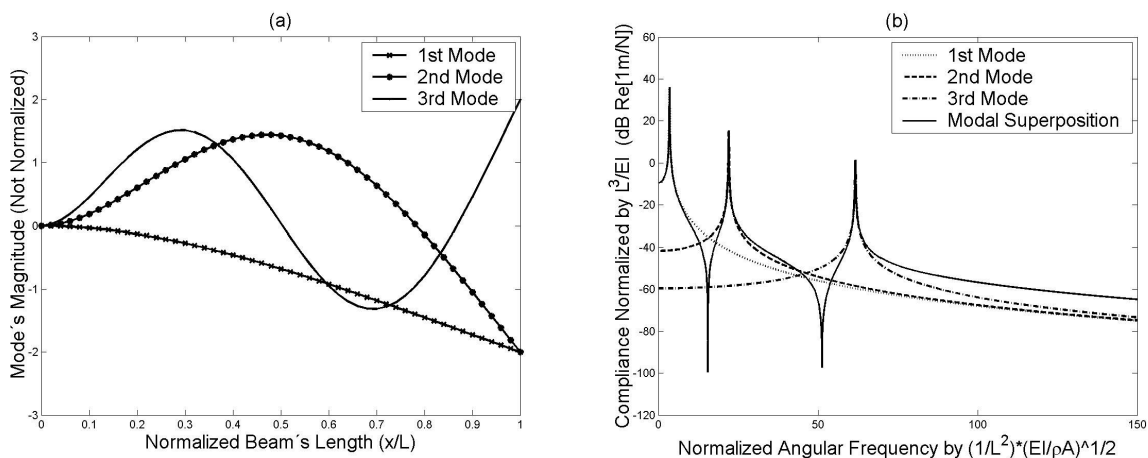


Figure 3 - Modal shape (a) and compliance at the free end (b) for clamped-free beam FE model

Using the same procedure applied in the analytical solution, the static compliance contribution of each mode and the sum of them obtained are shown in Tab. 2. Comparing these results with the values of Tab. 1, it can be observed that the results obtained with the finite element model are very close to those obtained with the analytical solution. It could

also be observed that the first mode contributes with 97% of the static compliance. Figure 4 presents the bar plot of the modal contribution in this case.

Table 2 – Modal static compliance - clamped-free beam FE model

Mode <i>r</i>	Static compliance for each mode ¹ $H_r(0,L,L)$	Compliance sum ¹ $\sum_{k=1}^r H_k(0,L,L)$
1	3.235627e-01	0.3235627
2	8.238610e-03	0.3318014
3	1.050822e-03	0.3328522
4	2.736497e-04	0.3331258
5	1.001415e-04	0.3332260
6	4.487642e-05	0.3332708
7	2.300507e-05	0.3332939
8	1.297910e-05	0.3333068
9	7.867424e-06	0.3333147
10	5.042432e-06	0.3333197

¹ - normalized using $\frac{L^3}{EI}$

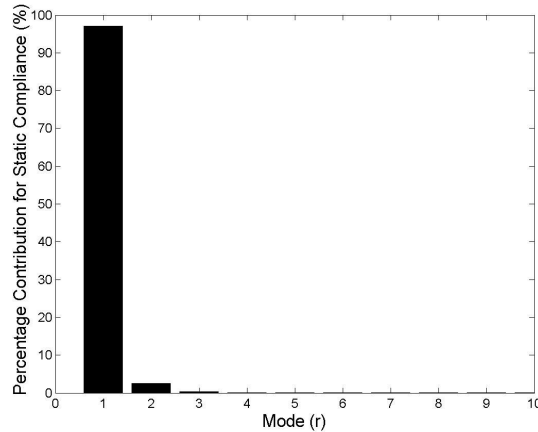


Figure 4 - Modal contribution to static compliance - clamped-free beam FE model

Free-Free Beam

Using the same FE mesh but now in the situation free-free, the modal shapes for the three first structural modes of the beam were gotten and they are shown in Fig. 5(a). Also, the compliance contributions for these modes at one of the free ends are shown in Fig. 5(b).

The interest in the study of the free-free case is due to the fact that this condition is the most used in experimental modal tests. This boundary condition is easy and fast to setup and, as a consequence, easier to reproduce. It will be shown that with the dynamic results obtained with the finite element model for the free-free beam it is possible to find the static stiffness values for the clamped-free beam just by handling the beam compliance at different degrees of freedom.

With this purpose, consider the clamped-free beam shown in Fig. 1. Assume that a force is applied at the free end in the transversal direction. This force will cause a vertical deformation throughout the beam and force and moment reactions at the clamped end. Figure 6(a) illustrates this situation. In this figure, point 1 corresponds to the clamped end of the beam and point 2 to the free end. F_1 is the force at point 1, F_2 is the force and M_2 is the moment at point 2 and Δy is the displacement at the free end position (dotted line). The following conventions were assumed: force and displacements are positive when pointing upwards, moments and angular displacements are positive in the counter-clockwise direction.

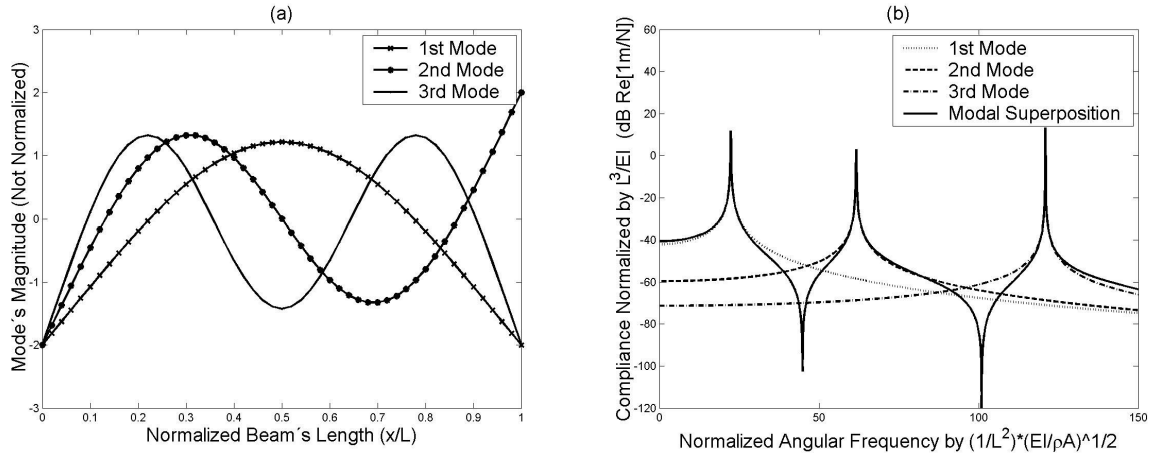


Figure 5 - Modal shapes (a) and free end compliance (b) for a free-free beam FE model

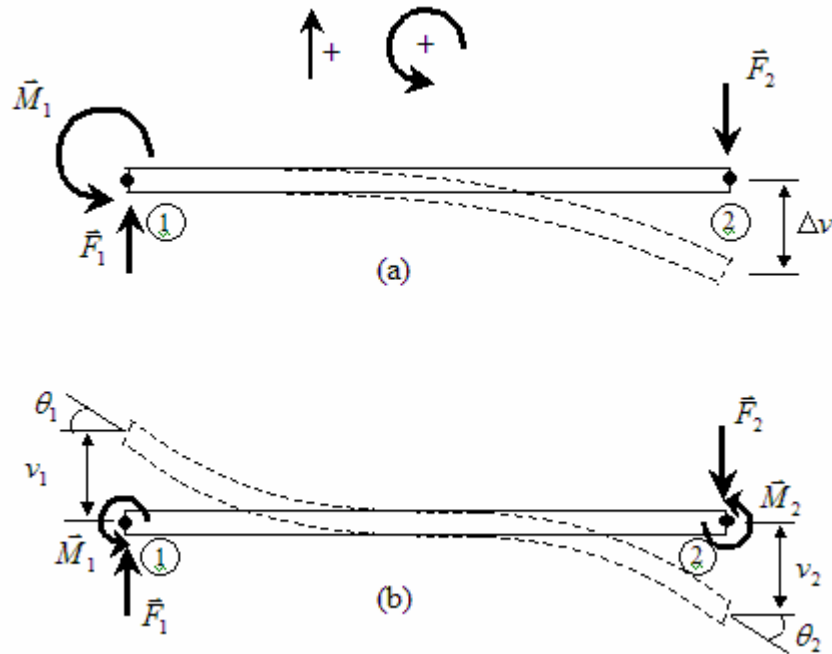


Figure 6 - Forces and moments acting on a clamped-free beam loaded in the free end (a) and sign notation for the efforts (b)

The free-free beam submitted to the set of action and reaction forces and moments is shown in Fig 6(a), and the sign convention for the efforts and linear and angular displacements is shown in Fig. 6(b). In this figure, v_1 and v_2 are the displacements caused by the application of forces F_1 and reaction F_2 , respectively; θ_1 and θ_2 are the element rotation angles and M_1 and M_2 are the moments acting at the beam ends, respectively.

The compliance H_{ij} , where i is the DOF output point (displacement or angle) and j is the point under the input (force or moment), for points 1 and 2 is synthesized in agreement with Eq. (14), using eigenvectors of displacement or rotation. The displacements v_1 and v_2 are calculated from the contribution of forces and moments:

$$\begin{cases} v_1 = H_{v_1v_1} F_1 - H_{v_1v_2} F_2 - H_{v_1\theta_1} M_1 \\ v_2 = -H_{v_2v_2} F_2 + H_{v_2v_1} F_1 + H_{v_2\theta_1} M_1 \end{cases} \quad (15)$$

and, since $M_2 = 0$, the rotation angle at point 1 is given by:

$$\theta_1 = H_{\theta_1v_1} F_1 - H_{\theta_1v_2} F_2 + H_{\theta_1\theta_1} M_1 \quad (16)$$

The deformation Δv of Fig. 6(a) can then be calculated:

$$\Delta v = v_2 - v_1 - \theta_1 L \quad (17)$$

Table 3 presents the results for the deformation Δv calculated from Eq. (17) using forces and moments of unitary magnitude and the contribution of each mode. In this case the 20 first modes were used in Eq. (15) and Eq. (16). The results in this table show that the convergence towards the theoretical value of the static compliance is slower than the ones verified in previous cases, and a larger number of modes is necessary to obtain the same accuracy. Nevertheless, the theoretical result can be obtained with good approximation. However, the modal contribution is more distributed in this case, with lower participation of first mode and greater participation of higher order modes. Also, we can note that the contribution of the two last modes does not keep the trend of monotonic fall and rise in relation to the previous modes. This effect is caused by the residual contribution of the modes not considered due to the FE discretization, i.e., they are a consequence of the truncation of a continuous model by a discrete one. Figure 7 shows these evidences in a graphical way.

Table 3 – Modal contribution to the beam end deflection obtained using a free-free FE model

Mode r	Static deformation for each mode ¹ Δv_r	Sum of modal deformations ¹ $\sum_{k=1}^r \Delta v_k$
1	1.725945e-01	0.1725945
2	3.612376e-02	0.2087182
3	3.314735e-02	0.2418656
4	1.483360e-02	0.2566992
5	1.355644e-02	0.2702556
6	7.987257e-03	0.2782429
7	7.462728e-03	0.2857056
8	4.999810e-03	0.2907054
9	3.897227e-03	0.2946027
10	2.837627e-03	0.2974403
11	3.571505e-03	0.3010118
12	3.036021e-03	0.3040478
13	3.047136e-03	0.3070949
14	2.604209e-03	0.3096992
15	2.526826e-03	0.3122260
16	2.101140e-03	0.3143271
17	1.763542e-03	0.3160907
18	8.853820e-04	0.3169760
19	8.432763e-03	0.3254088
20	7.924527e-03	0.3333333

¹ - normalized using $\frac{L^3}{EI}$

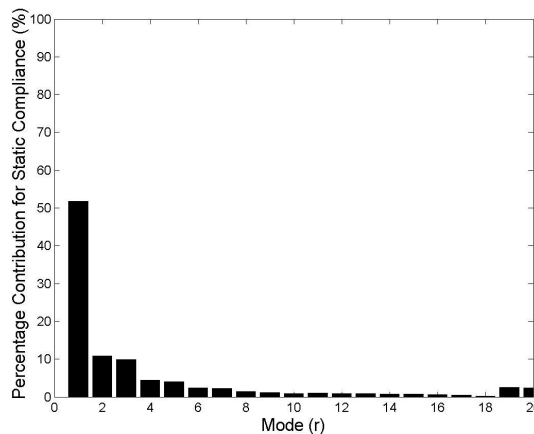


Figure 7 – Modal contribution to static deflection of the beam end calculated using a free-free FE model

CONCLUSION

The results shown in this paper demonstrate that information about the static compliance/stiffness of a structure can be extracted from a dynamic modal analysis. Moreover, it was shown that the restrictions necessary in static tests can be simulated through manipulation of the compliances obtained from a modal test under free-free condition. This

Obtaining Static Structural Stiffness from Modal Tests

possibility is particularly interesting in experimental tests where the free-free condition is easier to implement for a dynamic modal test. The dynamic tests are simpler to perform when compared with the static test procedures. Since both tests must be performed during the development of a structure, it is possible to save expenses only performing the dynamic one: different assemblies and replacement of sensors and actuators are prevented in static tests; results are calculated from the dynamic compliance matrix, synthesized between the different degrees-of-freedom of the structure. However, as a disadvantage, this method works considering only linear deformation.

This methodology is currently being applied to a 3D frame structure. With this purpose, we are implementing an FE model and performing static tests at present. Following that, an experimental modal analysis will be performed.

REFERENCES

- Chang, T., and Craig, R. R., Jr., 1969, *Normal Modes of Uniform Beams*, J. Eng. Mech. Div., EM4(95), pp1027-1031.
- Craig, R. R., Jr., 1981, *Structural Dynamics - An Introduction to Computer Methods*, John Wiley & Sons Inc.
- Ewins, D. J., 1984, *Modal Testing: Theory and Practice*, John Wiley & Sons Inc.
- Griffiths, D., Aubert, A., Green, E. R., and Ding, Jim, 2003, *A Technique for Relating Vehicle Structural Modes to Stiffness as Determined in Static Determinate Tests*, Noise & Vibration Conference and Exhibition - SAE.
- Rediers, B., Yang, B., and Juneja, V., 1998, *Static and Dynamic Stiffness: One Test, Both Results*, Proceedings of the International Modal Analysis Conference - IMAC, pp 30-35.

RESPONSIBILITY NOTICE (HEADING 1, HELVETICA 11PT BOLD ALL CAPS)

The authors are the only responsible for the printed material included in this paper.